Available online at www.sciencedirect.com

ScienceDirect

Ceramics International 41 (2015) 9265–9275

CERAMICS INTERNATIONAL

www.elsevier.com/locate/ceramint

Enhancement of ferromagnetic and ferroelectric properties in calcium doped $BiFeO_3$ by chemical synthesis

L.V. Costa[a,1], L.S. Rocha[a,1], J.A. Cortés[a,1], M.A. Ramirez[a,1], E. Longo[b,2], A.Z. Simões[a,*]

[a]*Universidade Estadual Paulista UNESP, Faculdade de Engenharia de Guaratinguetá, Av. Dr. Ariberto Pereira da Cunha, 333, Bairro Portal das Colinas, CEP 12516-410 Guaratinguetá, SP, Brazil*

[b]*Universidade Estadual Paulista-UNESP, Instituto de Química, Laboratório Interdisciplinar de eletroquímica e Cerâmica (LIEC), Rua Professor Francisco Degni s/n, Zip-Code 14800-90 Araraquara, SP, Brazil*

Received 23 January 2015; received in revised form 2 March 2015; accepted 14 March 2015
Available online 14 April 2015

Abstract

Calcium (Ca)-doped bismuth ferrite ($BiFeO_3$) thin films prepared by using the polymeric precursor method (PPM) were characterized by X-ray diffraction (XRD), atomic force microscopy (AFM), polarization and magnetic measurements. Structural studies by XRD and Rietveld refinement reveal the co-existence of distorted rhombohedral and tetragonal phases in the highest doped $BiFeO_3$ (BFO) where enhanced ferroelectric and magnetic properties are produced by internal strain. A high coercive field in the hysteresis loop is observed for the $BiFeO_3$ film. Fatigue and retention free characteristics are improved in the highest Ca-doped sample due to changes in the crystal structure of BFO for a primitive cubic perovskite lattice with four-fold symmetry and a large tetragonal distortion within the crystal domain.

Keywords: A. Ceramics; A. Thin films; B. Chemical Synthesis; D. Ferroelectricity

1. Introduction

Multiferroic materials with ferroelectric and ferromagnetic simultaneous ordering are currently attracting significant attention due to their interesting fundamental physics as well as their potential applications [1–5]. Among the single-phase multiferroic materials studied, $BiFeO_3$ (BFO) with a rhombohedrally distorted perovskite structure and a space group of R3c is the only material which exhibits both ferroelectricity and G-type antiferromagnetism at room temperature (with a Curie temperature Tc of 1103 K and Néel temperature T_N of 643 K) which facilitates applications at room temperature [6–8]. However, pure BFO has a serious high leakage current problem resulting from charge defects such as oxygen vacancies and the cancellation of ion magnetic moments due to its spatial periodic inhomogeneous spin structure [9] which hinders its practical applications in multiferroic devices. Considerable efforts have been expended to improve BFO properties; e.g., A-site substitution with La^{3+}, Nd^{3+}, Ce^{3+} and Tb^{3+} [10–15] and B-site substitution with Ni^{2+}, Cu^{2+}, Co^{2+}, Cr^{3+}, Mn^{3+}, Ti^{4+}, Zr^{4+} and V^{5+} [16–18] etc. These studies confirmed that ion doping is an effective method to improve BFO properties. Since ferroelectricity of BFO evolves from a lone pair of A-site Bi^{3+} ion electrons, ferroelectric property effects are very important [19–20]. Ramesh et al. studied the quasi-non-volatile and reversible modulation of electric conduction accompanied by the modulation of the ferroelectric state in Ca-doped $BiFeO_3$ films using an electric field as the control parameter. The mechanism of this modulation in Ca-doped $BiFeO_3$ is based on electronic conduction as a consequence of naturally produced oxygen vacancies that act as donor impurities to compensate Ca acceptors and maintain a highly stable Fe^{3+} valence state [21]. For the low Ca doping regime ($x < 0.1$), films with a

*Corresponding author. Tel.: +55 12 3123 2228; fax: + 55 12 3123 2868
E-mail addresses: joalcosu.nal@gmail.com (J.A. Cortés), alezirpoli@feg.unesp.br (A.Z. Simões).
[1]Tel.: +55 12 3123 2228.
[2]Tel.: +55 16 3301 9828.

http://dx.doi.org/10.1016/j.ceramint.2015.03.086
0272-8842/

monoclinic structure undergo a first-order transition to a pseudo-tetragonal phase at higher temperatures with a thermal hysteresis. The extrapolation of the transition temperature results in the well-known ferroelectric Curie temperature (T_c) of $BiFeO_3$ at 1100 K. With increased Ca doping, the ferroelectric T_c rapidly decreases, and a T_c of 600 K with a thermal hysteresis of 240 K is recorded. It has been reported that the T_c of some ferroelectrics such as $BaTiO_3$ and $PbTiO_3$ is very sensitive to the strain state [22,23]. However, because $BiFeO_3$ ferroelectricity is primarily attributed to Bi 6s lone-pair electrons, ferroelectric properties and the T_c are expected to be less sensitive to strain [24]. Many of these studies were focused on improving the electrical and magnetic properties of BFO. Compared with magnetic property, significant achievements were gained in improving electrical property of BFO [25,26]. Therefore, we throw our light mainly on investigating the magnetic property of BFO in this paper, noted that substitutions of Pr^{4+},Ce^{3+}, Zr^{4+} and Ca^{2+} for partial Bi^{3+} at A-site had improved the magnetic properties of BFO to different extent [27–31], and Ca^{2+} was shown to be the best substitution for enhancing the saturation magnetization. However, there is still no agreement on the mechanism of how the magnetic properties of BFO are affected by now [32–34]. Ederer et al. [35] and Ueda et al. [36] thought that both Fe ions and oxygen vacancy help to improve the magnetic property of BFO to some extent. In most applications involving ferroelectric films, there are several parameters to technological adoption, such as fatigue-endurance, remnant polarization (2Pr), coercive field (2Ec), and processing temperature [37,38]. Recently, changes in the crystal structure of BFO for a primitive cubic perovskite lattice with four-fold symmetry and a large tetragonal distortion within the crystal domain were attained for ferroelectric Ca-doped samples. This observation introduces magnetoelectronics at room temperature by combining electronic conduction with electric and magnetic degrees of freedom which are already present in the multiferroic $BiFeO_3$. A comparative study shows that A-site Ca doping with various contents have notable influences on electrical properties, including leakage current and ferroelectric and piezoelectric properties of BFO films which may be related to modification of the structure and elimination of charge defects due to A-site Ca doping [39]. However, the fatigue and retention characteristics of A-site Ca doping films have so far not been reported by the polymeric precursor method. In a memory element, a data bit (1 or 0) should be stored and made available for query at some later time. Retention is the ability of a memory element to maintain a given data state as time elapses. In most retention studies, ferroelectric capacitors exhibited a significant loss in retained polarization within the first one second after writing and then a relatively slight decay thereafter [40]. Retention loss causes a reduction in the difference between switched (P^*) and non-switched ($\hat{P}$) polarizations, i.e $\Delta P=(P^*)-(\hat{P})$ and leads to an inability to distinguish between the two logic states. Therefore, it is quite important to have good retention properties for any ferroelectric material to be utilized for FRAM applications. In this paper, we report the first systematic studies on the fatigue and retention characteristics of A-site Ca doping thin films obtained by the polymeric precursor method. We have also investigated the enhancement magnetism for A-site Ca-doped BFO films with different compositions on $Pt/Ti/SiO_2/Si$ substrates by using the PPM method.

2. Experimental procedure

$BiFeO_3$ (BFO) and $Bi_{1-x}Ca_xFeO_3$ with $x=0.10$ (BCF010); 0.20(BCF020); 0.30 (BCF030) thin films were prepared by the PPM as described elsewhere [40], using Iron (III) nitrate nonahydrate, (99.5% purity, Merck), Bismuth nitrate ($\geq$99% purity, Aldrich) and Calcium carbonate (99.9% purity, Aldrich) as raw materials. An excess of 5 wt% Bi was added to the solution to minimize bismuth loss during thermal treatment. Films were spin coated on $Pt/Ti/SiO_2/Si$ substrates by a commercial spinner operating at 5000 revolutions/min for 30 s (spin coater KW-4B, Chemat Technology). Thin films were annealed at 500 °C for 2 h in a conventional furnace under static air atmosphere. The film thickness was reached by repeating spin-coating and heating treatment cycles ten times. Annealed film thicknesses were measured using SEM (Topcom SM-300) at the transversal section. We have obtained films with thicknesses in the range of 340 to 360 nm. A phase analysis of films was performed at room temperature by XRD using a Bragg-Brentano diffractometer (Rigaku 2000) and Cu-Kα radiation; in this case, back scattering electrons were used. The Rietveld analysis was performed with the Rietveld refinement program DBWS-941 1 [41]. The profile function used was the modified Thompson-Cox-Hastings pseudo-Voigt where η (the Lorentzian fraction of the function) varies with the Gauss and Lorentz components of the full width at half maximum. The surface morphology of the thin films was measured by atomic force microscopy (AFM) using a tapping mode technique. Top Au electrodes (0.5 mm diameter) were prepared for electrical measurements by evaporation through a shadow mask at room temperature. The capacitance–voltage characteristic was measured in the MFM configuration using a small AC signal of 10 mV at 100 kHz. The AC signal was applied across the sample, while the DC was swept from positive to negative bias. Ferroelectric properties of the capacitor were measured on a Radiant Technology RT6000 instrument and a tester equipped with a micrometer probe station in a virtual ground mode at a frequency of 60 Hz. These loops were traced using the Charge 5.0 program included in the software of the RT6000HVS in a virtual ground mode test device. For the fatigue measurements, internally generated 8.6 μs wide square pulses were used. After the end of each fatigue period, the polarization characteristics of the films were measured over a range of frequencies. Retention characteristics of the films were measured by independently observing the time-dependent changes of P^* (switched polarization), and $\hat{P}$ (nonswitched polarization). For P^*, the capacitor was switched with a negative write pulse and read by a positive read pulse after retention time t. For $\hat{P}$, positive pulses were used for both writing and reading. The pulse width for all triangular pulses was 1.0 ms. The time delay between the written pulse and the first read pulse is referred to as retention time.

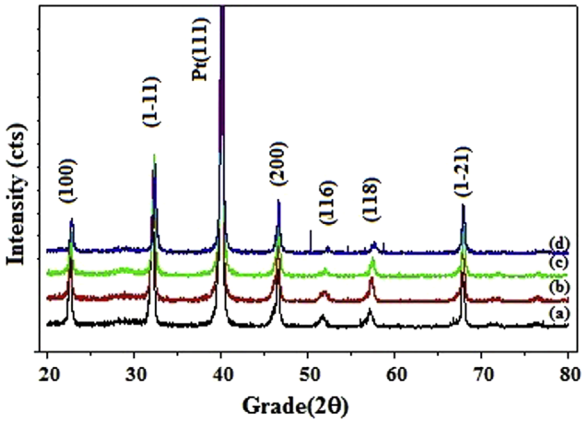

Fig. 1. X-ray diffraction of (a) BFO, (b) BFOCa010, (c) BFOCa020, (d) BFOCa030 thin films deposited by the polymeric precursor method and annealed at 500 °C in static air for 2 h.

Magnetization measurements were done by using a vibrating-sample magnetometer (VSM) from Quantum Design™. All measurements were performed at room temperature.

3. Results and discussion

Fig. 1 illustrates XRD patterns of BFO and Ca-doped BFO films deposited on platinum-coated silicon substrates. The films were well crystallized at a processing temperature of 500 °C. BFO and Ca-doped BFO films self-organized to produce (110)-preferred orientation with good crystallinity. With partial substitution of Ca ions for A-site bismuth ions, the BCFO film (108) diffraction peak shifted toward a higher angle. The BCF030 film has a tetragonal structure with a *P4mm* space group while BFO has a rhombohedral structure with an *R*3*c* space group which can be treated as a special triclinic structure [14]. However, the presence of impurity phase, such as $Bi_2Fe_4O_9$ was detected in addition to the major BFO phase. To verify and confirm the structure of BCFO thin films, a structural refinement by the Rietveld method was performed (Fig. 2a and b). The Rietveld method is a least squares refinement procedure where the experimental step-scanned values are adapted to calculated values. The profiles are considered to be known, and a model for a crystal structure is available [42]. This structural refinement method presents several advantages over conventional quantitative analysis methods because this method uses a whole pattern fitting algorithm where all lines for each phase are explicitly considered, and even severely overlapped lines are usually not a problem. Thus, it is not necessary to decompose patterns into separate Bragg peaks as is often the case for traditional methods. The use of all reflections in a pattern rather than just the strongest reflections minimizes both uncertainty in derived weight fractions and effects of preferred orientation, primary extinction and nonlinear detection systems [43]. The structural refinement was performed by using the Maud program [44] which employs the Rietveld texture and stress analysis [45]. According to the literature [46,47], the quality of data from structural refinement is generally checked by *R*-values (R_{wp}, R_{exp}, and *S*). The quality of structural refinement also can be verified by the R_{wp} factor value. Its absolute value does not depend on the absolute value of the intensities; instead it depends on the background, with a high background it is easier to reach very low values. Increasing the number of peaks (sharp peaks) creates more difficulty in obtaining a good value. Structural refinement data are acceptable when the R_{wp} is $< 10\%$ for a medium complex phase, when high complex phases (monoclinic to triclinic), have a value of $R_{wp} < 15\%$ and when a highly symmetric material or compound (cubic) with few peaks has a value of $R_{wp} < 8\%$ [48]. Table 1 lists R_{wp}, R_{exp}, and S indexes as well as lattice parameters (*a* and *c*) and the unit cell volume (V). Quantitative phase analyses of powders for the rhombohedral phase were calculated according to Young and Wiles [41] and the results obtained confirm that the Bi^{+3} ion was substituted by the Ca^{+2} ion in the rhombohedral BFO phase, and no changes occurred in refinements. Ca^{2+} replaces Bi^{3+} only in a perovskite-type unit cell which causes a distorted structure whereby distortion increases with a higher Ca content. The covalent interaction which originates from the strong hybridization between Fe 3*d* and O 2*p* orbitals plays an important role in the structural distortion of the BFO lattice. From low S values ($S = R_{WP}/R_{exp}$), it can be assumed that the refinement was successfully performed with all the investigated parameters close to literature data [49]. It can be inferred that the *c*-axis is less elongated after Ca addition which is caused by differences in charge densities of Ca and Bi atoms. Also, the addition of Ca has a radial substitution effect higher than bismuth and stabilizes oxygen vacancies and consequently the structure. The decrease in the lattice parameter and unit cell volume is almost linear as expected due to the stoichiometric replacement of Bi^{3+} with a smaller ionic radii substituent (in this case Ca^{2+}). The results obtained from the structural refinement are displayed in Table 1. In this table, the fitting parameters (R_{wp}, R_{exp}, and *S*) indicate good agreement between refined and observed XRD patterns. Small variations in lattice parameters and unit cell volumes are indicative of distortions/strain in the lattice caused by differences in crystal lattice parameters and in thermal expansion behavior between the film and the underlying substrate, or even arising from defects promoted by $[BiO_{12}]$ and $[CaO_{12}]$ clusters (network modifiers).

The surface morphology of the BFO and Ca-doped BFO thin films was evaluated by AFM measurements (Fig. 3). AFM studies demonstrated that Ca as a dopant reveals a homogeneous surface indicating that the soft chemical method allows the preparation of films with controlled morphology. Changes in the surface of the Ca-doped BFO films were evaluated and the results reveal that the BCF030 film consist of a homogeneous surface although BFO film has a degree of porosity. It was also found that the Ca dopant tends to suppress grain growth. BCF030 was found to be effective in improving the surface morphology of synthesized BFO-based films because the precursor film underwent the optimized nucleation and growth process to produce films with a homogeneous and dense microstructure. On the other hand, for low and middle Ca concentrations, the surface consists of irregularities which

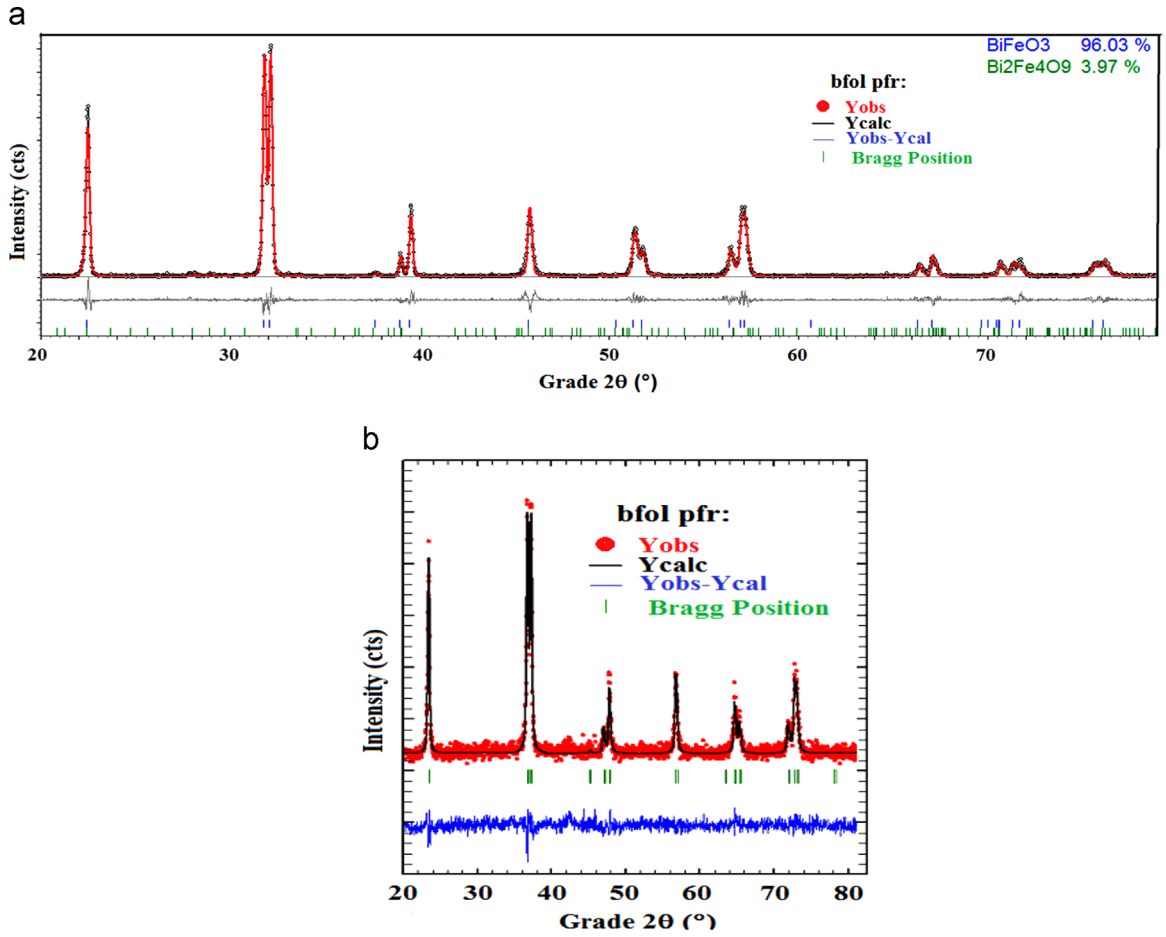

Fig. 2. Rietveld plots of (a) BFO and (b) BFOCa030 thin films deposited by the polymeric precursor method and annealed at 500 °C in static air for 2 h.

Table 1
Index refinements for BFO, BFOCa010, BFOCa020 and BFOCa030 thin films annealed at 500 °C for 2 h.

Refinement index	Parameter	**BFO**	**BFOCa010**	**BFOCa020**	**BFOCa030**
	R_{wp} (%)	8.14	5.97	5.51	4.59
	R_{exp}	4.67	3.91	3.76	3.31
	S	1.74	1.52	1.46	1.38
Lattice parameter	a (Å)	5.577352	5.576058	5.577687	5.578439
	c (Å)	13.867785	13.807185	13.773235	13.764944
	V (Å^3)	373.529	371.784	371.086	370.963
	t	0.915	0.916	0.919	0.920
Perovskite (mol%)		97.5 ± 0.5	97.1 ± 0.4	98.4 ± 0.4	97.7 ± 0.4
Stoichiometry		$BiFeO_3$	$Bi_{0.9}\ Ca_{0.1}FeO_3$	$Bi_{0.80}\ Ca_{0.2}FeO_3$	$Bi_{0.70}\ Ca_{0.30}FeO_3$
Refinement		$BiFeO_{2.6}$	$Bi_{0.9}\ Ca_{0.1}FeO_{2.6}$	$Bi_{0.80}\ Ca_{0.2}FeO_{2.6}$	$Bi_{0.70}\ Ca_{0.30}FeO_{2.8}$

were caused by distortion in the lattice caused by Ca addition. The average grain size is 63 nm for the BFO film and 33 nm for the highest doped film. The substitution of Ca^{2+} for Bi^{3+} in $BiFeO_3$ can produce oxygen vacancies which apparently induce distortions and causes structural irregularities within the crystallites. Also, the homogeneous microstructure of BCF030 films may affect ferroelectric properties because the voltage can be uniformly applied on them. The average surface roughness value is 6.2 nm for the BFO thin film, 6.1 nm for the BCF010 film, 5.8 nm for the BCF020 film and for the BCF030 film consists of a statistical roughness with a root mean square (RMS) of approximately 5.5 nm.

Fig. 4 illustrates the *C–V* curves obtained at 100 kHz and DC sweep voltage from +10 to −10 V. The dependence between capacitance, measured in nF, and voltage is strongly nonlinear, confirming the ferroelectric properties of the film resulting from domain switching. Non-symmetric *C–V* curves around the zero bias axis is evidenced with increasing calcium concentration indicating that the films contain movable ions or charge accumulation at the film–electrode interface. The *C–V*

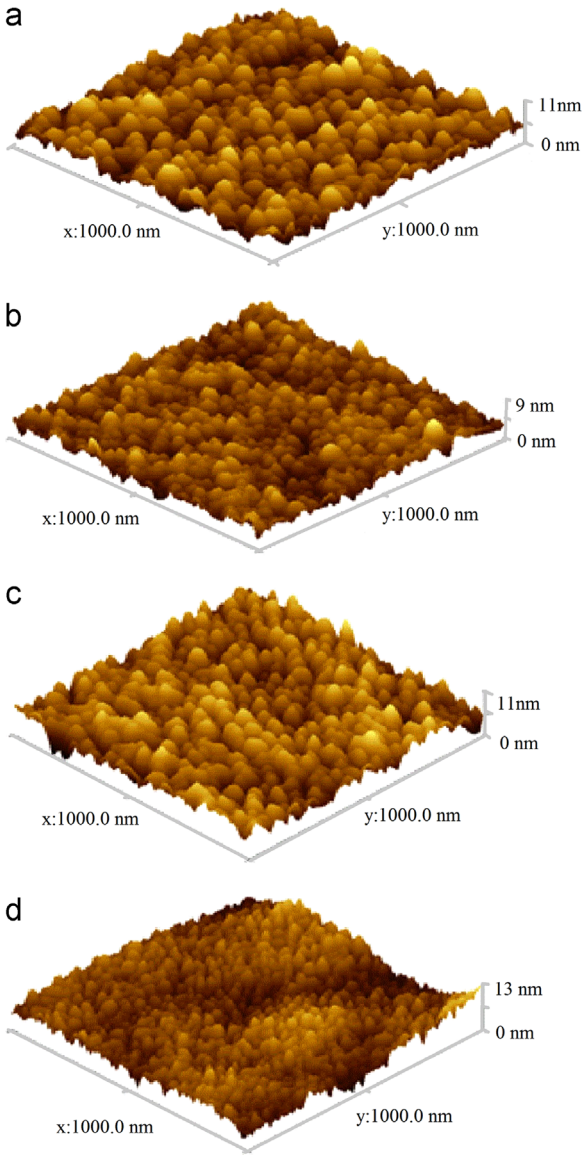

Fig. 3. AFM micrographies of thin films deposited by the polymeric precursor method and annealed at 500 °C in static air for 2 h. (a) BFO, (b) BFOCa010, (c) BFOCa020 and (d) BFOCa030.

curve shows hysteresis up to ± 10 V although the *P–E* hysteresis is saturated at ≥ 15 V because both measurements were performed at different frequencies where the domain alignment is a time dependent process and plays an important role in the switching behavior of the domains. Therefore, the sweep voltage ranges differ greatly and consequently also the (*dV*/*dt*) voltage sweep per time unit leading to different domain alignment kinetics.

Room temperature *P–E* hysteresis loops of BFO and Ca-doped BFO films are shown in Fig. 5. The BFO loop is well saturated and rectangular with a remnant polarization (Pr) of 51 μC/cm^2 under a voltage of 50 V. No sign of leakage has been observed under this measuring frequency. Liu et al. [50] reported substantially reduced leakage of $BiFeO_3$ films by introducing a $LaNiO_3$ intermediate layer. Although a saturated hysteresis loop was observed, they obtained only a remnant polarization of 26.9 μC/cm^2 under 1.25 MV/cm. To our knowledge, very few reports on a large *P*r and a rectangular loop of BFO film obtained from chemical methods [51,52] have been reported. However, the hysteresis loop in our study is more saturated than some BFO films on the Pt bottom electrode by the CSD method. In fact, pure BFO film loops on the Pt bottom electrode are unsaturated in some cases. Gonzalez et al. [40] observed saturated hysteresis loops at room temperature in pure BFO films on a Pt bottom electrode while they observed only a small remnant polarization ~36 μC/cm^2 under 800 kV/cm. In other typical studies from Singh et al. [53], Hu et al. [54] and Uchida et al. [55], unsaturated loops were observed under 10 kHz at room temperature. Our results are comparable to results observed in epitaxial BFO films on a (100) $SrTiO_3$ substrate prepared by the PLD method. The film possesses well saturated hysteresis characteristics with a remnant polarization (*Pr*) of 31 μC/cm^2 and a coercive field (*Ec*) of 560 kV/cm with a maximum applied electric field of 1000 kV/cm. According to Wang et al. [56], the BFO ferroelectricity originates from relative displacements of a Bi ion and a Fe–O octahedron along the (111) orientation in epitaxial BFO thin films, and the projection polarization along the (110) orientation is larger than the (100) orientation polarization. Imprint phenomena which cause a significant shift along the electric field axis toward the positive side is also evident in low and middle Ca-doped BFO as a consequence of oxygen vacancy accumulation near the electrode-film interface which reduces the effective applied electric field. The BCFO30 film presents a symmetric hysteresis loop which is indicative that calcium stabilizes the charged domain walls which interact with oxygen vacancies and reduce the coercive field. The imprint free phenomenon probably originates from the local distortion caused by the rhombohedral co-existing phase and is reflected in physical properties of the tetragonal phase. Adding Ca^{2+} ions to BFO in high concentrations requires charge compensation which can be achieved by the formation of Fe^{4+} or oxygen vacancies. If Fe^{4+} exists, the statistical distribution of Fe^{3+} and Fe^{4+} ions in the octahedron may also lead to strong polarization while high coercivity can be caused by the pinning of ferroelectric domain walls which results from the ferroelectric anisotropy.

When a ferroelectric material is repeatedly cycled from one polarization state to another, its dielectric and ferroelectric properties are observed to change. This phenomenon, known as ferroelectric fatigue, is a limiting factor for the performance of the ferroelectric random access memory (FRAM) devices. The fatigue endurance of pure and Ca doped BFO thin films were tested at 1 MHz as a function of switching cycles by applying 8.6 μs wide bipolar pulses with maximum amplitudes of ± 9 V (Fig. 6). P^* is the switched polarization between two opposite polarity pulses and $\hat{P}$ is the nonswitched polarization between the same two polarity pulses. The $P^*-\hat{P}$ or $-P^*-(-\hat{P})$ denote the switchable polarization, which is an important variable for nonvolatile memory application. We claim that calcium stabilizes the charged domain walls which

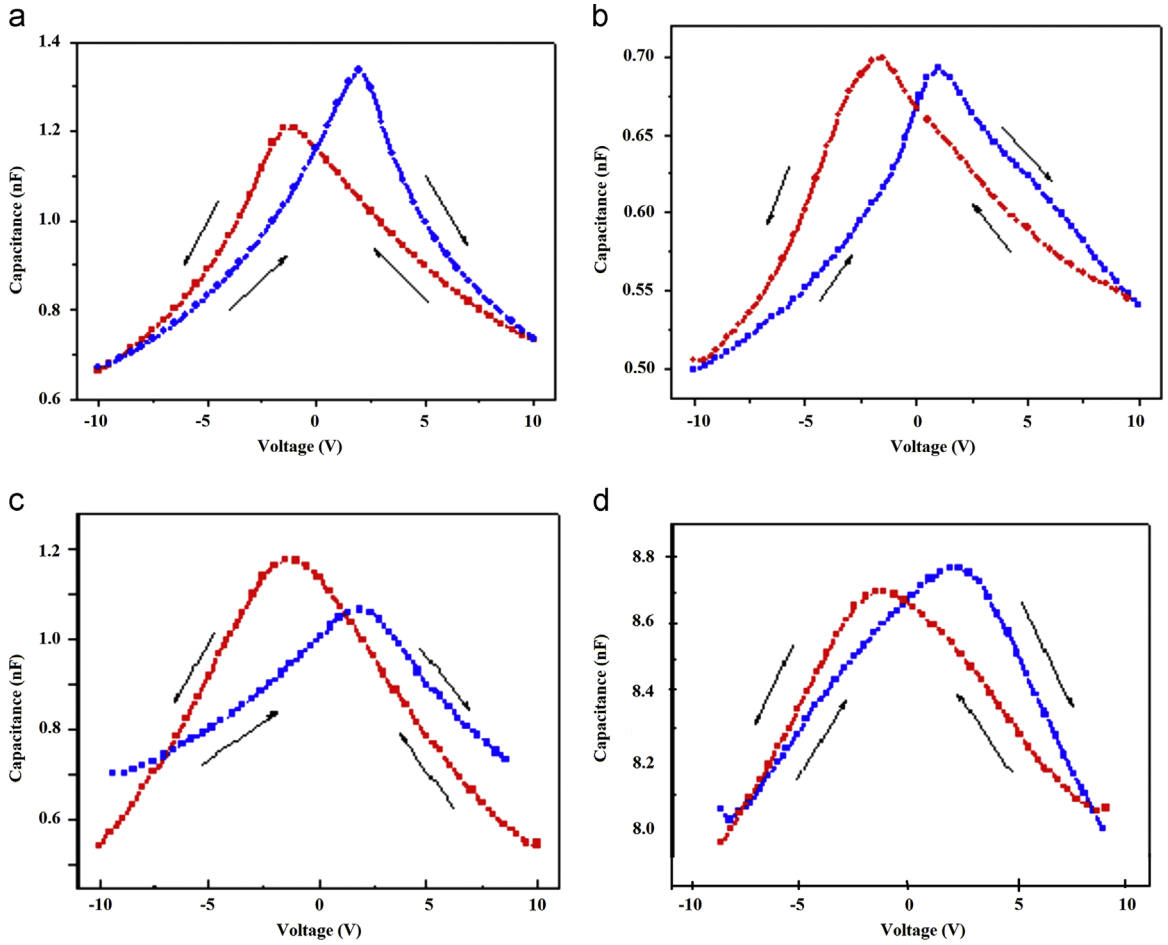

Fig. 4. Capacitance–voltage curves of thin films deposited by the polymeric precursor method and annealed at 500 °C in static air for 2 h. (a) BFO, (b) BFOCa010, (c) BFOCa020 and (d) BFOCa030.

interact with oxygen vacancies and inhibit fatigue. During fatigue, an accumulation of oxygen vacancies near the electrode-film interface can occur, which reduces the effective applied electric field. This fact is well-reflected in fatigue measurements (Fig. 6a–d), that clearly show that even after 10^{10} switching cycles, no decay in the remnant polarization is present for the heavily Ca-doped samples ($x=0.20$ and $x=0.30$). The substitution of Ca for Bi can change the chemical environment of the perovskite layers and solve the fatigue problem of pure BFO thin films. Since a Ca^{3+} ion has no outer electron, in contrast to a Bi^{3+} ion, which has a lone pair of 6*s* electrons, less hybridization with O 2*p* should lead to less structural distortion favoring the improvement of its ferroelectric properties. The maximum amplitude of 9 V was applied to all films taking into account that the BCFO30 film presents low coercitive field which is employed as a tool for fatigue endurance.

Retention, which is the time dependent change of the polarization state of the ferroelectric film, is another factor which limits the life of a ferroelectric memory device. Ferroelectric retention properties were measured at room temperature using a Radiant Radiant Technology RT6000 A test system (Fig. 7). The test pulse sequence used for retention measurement is as follows: at first, a triangular pulse of −5 V was applied to write a known logic state, then, after a predetermined time, the logic state was sequentially read by applying two triangular pulses of +5 V and −5 V. The pulse width for all triangular pulses is 1.0 ms. Time delay between the right pulse and the first read pulse is called the retention time. The capacitor poled with a negative voltage pulse corresponds to the binary digit "1". Similarly the state "0" was written by poling the capacitor by applying a positive pulse and read after a predetermined time interval r with a positive pulse. Fig. 7a shows the retention characteristics of the BFO films, where the retained switchable polarization $\Delta P = (P^*) - (\hat{P})$ was plotted as a function of retention time from 1 s to 1×10^4 s at a applied electric field of 150 kV/cm. The value of initial polarization decayed and approached a nearly steady-state value after a retention time of 10 s. The corresponding hysteresis loops obtained after the retention test was also essentially identical to that observed before the retention test, indicating that the switchable polarization has almost no loss and the structures have little or no tendency to imprint after 1×10^4 s. The small decay of the retained charge in Ca-doped BFO thin films even after about 1×10^4 s is a favorable indication for memory applications. The long-time retention characteristics of the Ca-doped BFO thin films are shown in

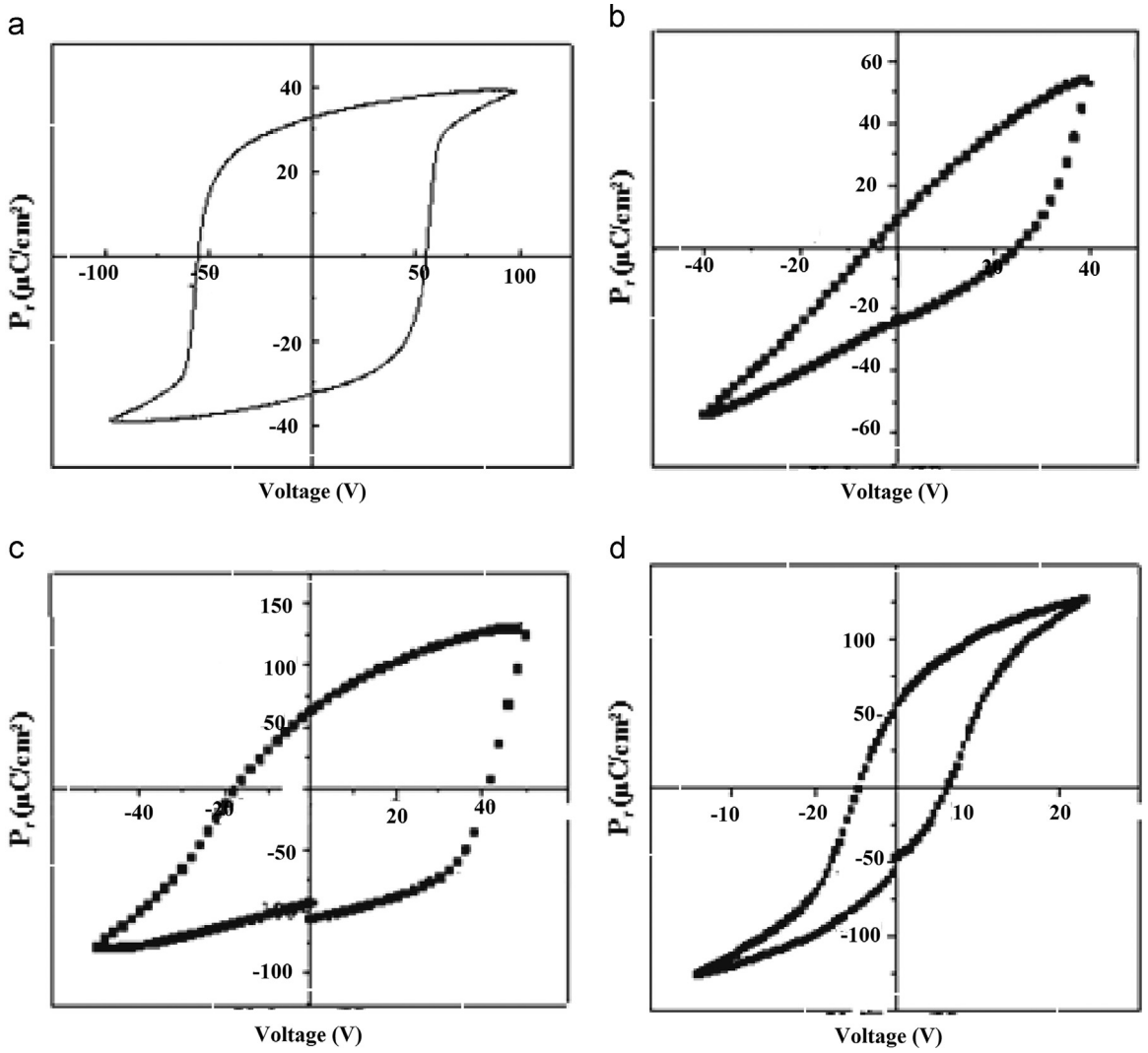

Fig. 5. Hysteresis loop of thin films deposited by the polymeric precursor method and annealed at 500 °C in static air for 2 h. (a) BFO, (b) BFOCa010, (c) BFOCa020 and (d) BFOCa030.

Fig. 7b. The overall retention time dependence of polarization retention for the BFOCa030 film is quite good. After a retention time of 1×10^4 s, the polarization loss was only about 6% of the value measured at $t = 1$ s for an applied electric field of 150 kV/cm. Depolarization fields generated by the redistribution of space charge, defects and dipole charges could be the mechanisms for the polarization decay after writing. For the infant period (within 10 s), depolarization fields could be the main contribution to polarization loss. The depolarization field increases with increasing the retained polarization and is time dependent. The long-time retention loss is attributed to the effects of redistribution of defect charges. This effect leads to a small decrease in the polarization by compensating the polarization charges when the redistribution of defect charges is driven by polarization. Due to the dielectric relaxation, the retained charge is generally less than the switched charge measured from the *P-E* hysteresis loop and the difference between them should be small as possible to keep enough margin between the digits "1" and "0". Retention, like fatigue, is also dependent on the thickness of the film, nature of the electrodes, microstructure of the film, temperature, and the details of the test conditions. The understanding and improvement of the degradation behavior of ferroelectric thin films will have an essential impact on the future success of these films for device applications. Detailed fatigue and retention measurements in close correlation with process conditions are being done to evaluate the merits of calcium bismuth ferrite thin films for memory applications.

The magnetic hysteresis loops, as shown in Fig. 8(a–c), illustrate the non-linear field dependence of magnetization *M* for pure BFO indicating its AFM nature. However, highest Ca-doped film is ferromagnetic at RT and the characteristics of the loop depend on concentration of calcium. Reminiscent magnetization and coercivity are maximum in the case of BFOCa030. Although the reason behind the occurrence of FM in Ca-doped BFO samples is not clearly understood, this can be attributed to the change in interaction between Fe^{+3} and Fe^{+4}

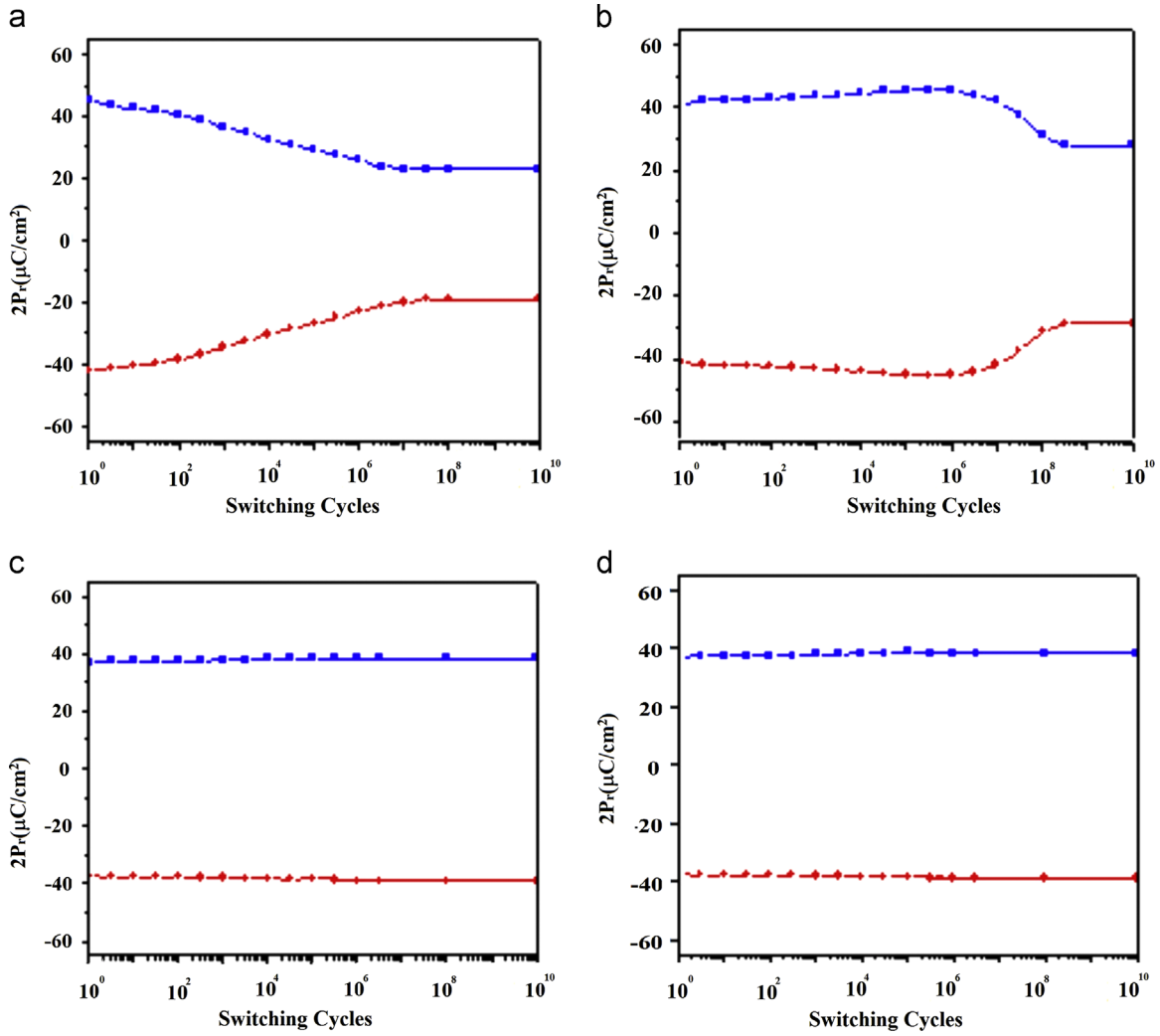

Fig. 6. Fatigue behavior of thin films deposited by the polymeric precursor method and annealed at 500 °C in static air for 2 h. (a) BFO, (b) BFOCa010, (c) BFOCa020 and (d) BFOCa030.

breaking down the balance between the antiparallel sublattice magnetization [10]. Change in canting angle [34] or spiral spin modulation [56] may also be responsible for this phenomenon. The saturation magnetization (Ms) of the BFOCa030 films were about 2.5 emu/g, higher than those of reported La-doped or Cr-doped [17] BFO films (Fig. 8d). This indicated that the magnetization of the films was remarkably enhanced by substitution of Ca^{2+} for Bi^{3+}. Ederer et al. [35] and Ueda et al. [36] thought that both Fe ions and oxygen vacancy help to improve the magnetic property of BFO to some extent. Other studies [56–58] indicated that the magnetic properties of $BiFe_{1-x}Ti_xO_3$, $Bi_{0.88}La_{0.2}FeO_3$ and $BiFe_{1-x}Sc_xO_3$ were significantly affected by Fe^{2+} ion. The Fe^{2+} ion in BFO was believed to be related to the formation of oxygen vacancy, while oxygen vacancy was thought as one of the important causes for leakage current in BFO [59,60]. The Fe^{2+} ion in BFO was believed to be related to the formation of oxygen vacancy, while oxygen vacancy was thought as one of the important causes for leakage current in BFO. XPS studies are ongoing to elucidate the valence state of iron in the undoped and Ca doped samples.

4. Conclusions

In summary, the effect of divalent-ion-Ca doping on multiferroic $BiFeO_3$ films was investigated on a Pt substrate using the soft chemical method through annealing at 500 °C for 2 h. The highest Ca concentration changes the local distortion and strain caused by the rhombohedral co-existing phase which is reflected in physical properties of the system. Among these films studied, the BCFO30 film exhibited a better microstructure, a good *P–E* loop, fatigue and retention free behavior as well as better magnetic response. Calcium improved the fatigue and ferroelectric properties of the films changing the structure from rhombohedral to tetragonal. The retention failure tests showed that the Ca-doped BFO films have quite good long-time retention characteristics, retaining 94% of the values measured at $t = 1 \times 10^4$ s for an applied electric field of 150 kV/cm. Polarization charge compensation by the redistribution of defect charges should be considered to explain the retention loss in calcium doped bismuth ferrite thin films for memory applications. The results of these studies are very

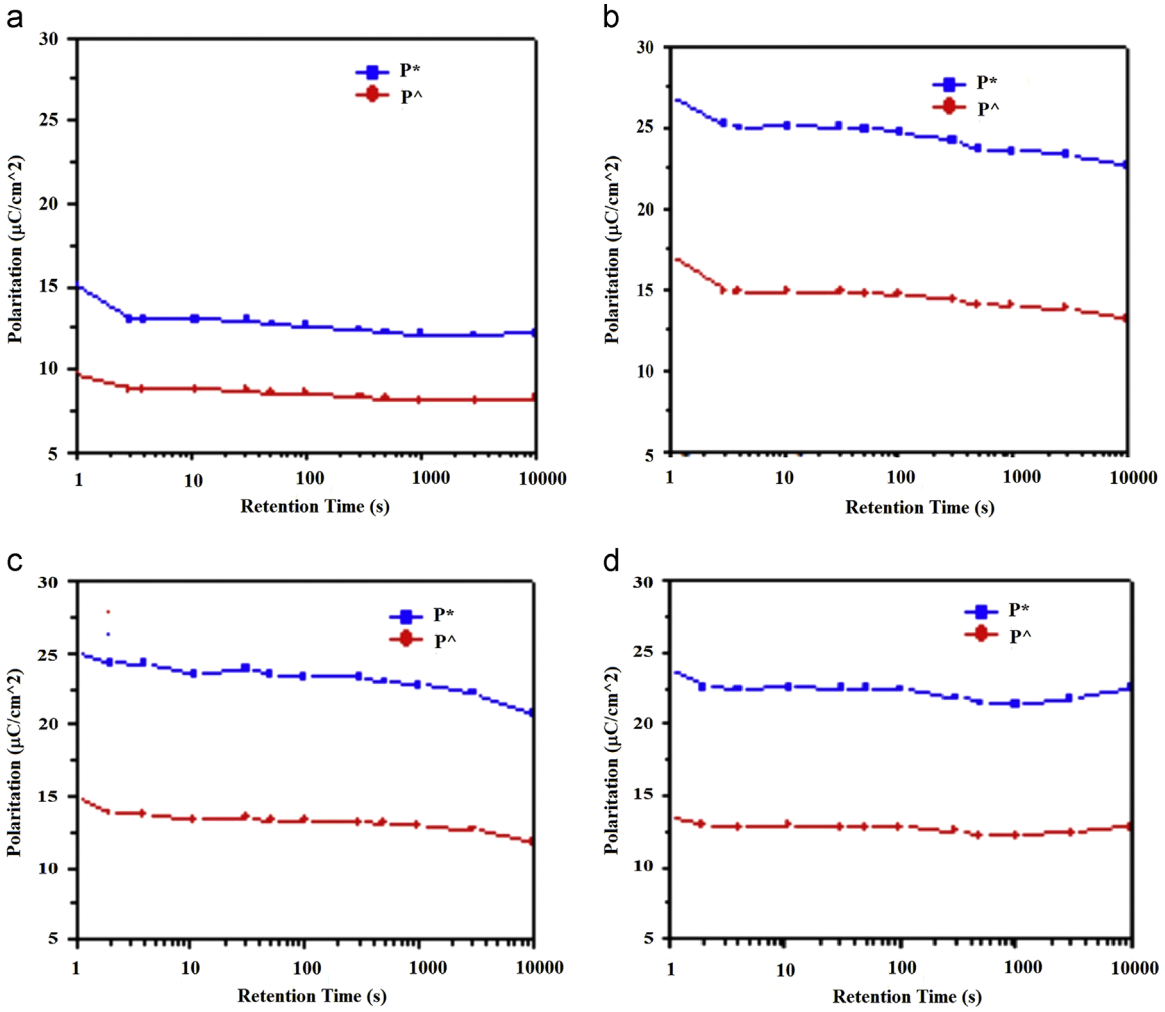

Fig. 7. Retention characteristics of thin films deposited by the polymeric precursor method and annealed at 500 °C in static air for 2 h. (a) BFO, (b) BFOCa010, (c) BFOCa020 and (d) BFOCa030.

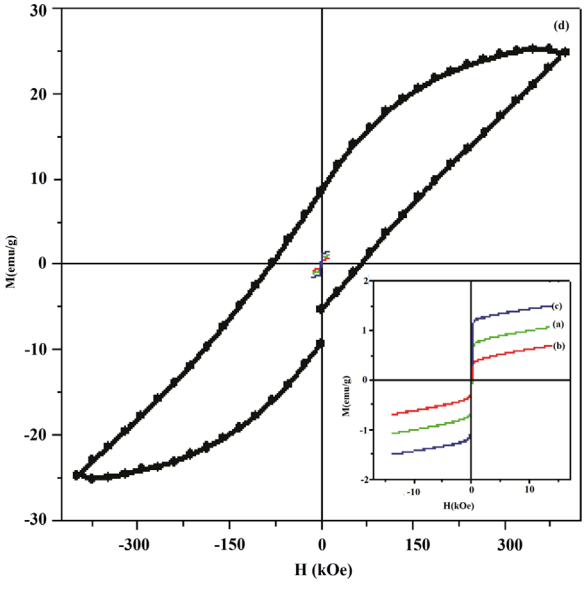

Fig. 8. Magnetic behavior of thin films deposited by the polymeric precursor method and annealed at 500 °C in static air for 2 h. (a) BFO, (b) BFOCa010, (c) BFOCa020 and (d) BFOCa030.

promising and suggest that BCFO30 thin films are attractive for use as storage element in non-volatile ferroelectric and magnetic random access memories.

Acknowledgments

The financial support of this research project by the Brazilian Research funding agencies CNPq 573636/2008-7, INCTMN 2008/57872-1 and FAPESP 2013/07296-2.

References

[1] J. Wang, J.B. Neaton, H. Zheng, V. Nagarajan, S.B. Ogale, B. Liu, D. Viehland, V. Vaithyanathan, D.G. Schlom, U.V. Waghmare, N.A. Spaldin, K.M Wuttig, R. Ramesh, Epitaxial $BiFeO_3$ multiferroic thin film heterostructures, Science 299 (2003) 1718.

[2] W. Eerenstein, F.D. Morrison, J. Dho, M.G. Blamire, J.F. Scott, N.D. Mathur, Comment on epitaxial $BiFeO_3$ multiferroic thin film heterostructures, Science 307 (2005) 1203a.

[3] L.W. Martin, S.P. Crane, Y.H. Chu, M.B. Holcomb, M. Gajek, M. Huijben, C.H. Yang, N. Balke, R. Ramesh, Multiferroics and magnetoelectrics: thin films and nanostructures, J. Phys. Condens. Matter 20 (2008) 434220.

[4] G. Catalan, J.F. Scott, Physics and applications of bismuth ferrite, Adv. Mater. 21 (2009) 2463.

[5] K.F. Wang, J.M. Liu, Z.F. Ren, Multiferroicity, the coupling between magnetic and polarization, Adv. Phys. 58 (2009) 321.

[6] G.A. Smolenskii, I.E. Chupis, Ferroelectromagnets, Sov. Phys. Usp. 25 (1982) 475.

[7] I. Sosnowska, T. Peterlin-Neumaier, E. Steichele, Spiral magnetic ordering in bismuth ferrite, J. Phys. C Condens. Matter 15 (1982) 4835.

[8] C. Ederer, N.A. Spaldin, Weak ferromagnetism and magnetoelectric coupling in bismuth ferrite, Phys. Rev. B 71 (2005) 060401.

[9] X.D. Qi, J. Dho, R. Tomov, M.G. Blamire, J.L. MacManus-Driscoll, Greatly reduced leakage current and conduction mechanism in aliovalent-ion-doped $BiFeO_3$, Appl. Phys. Lett. 86 (2005) 062903.

[10] F.Z. Huang, X.M. Lu, W.W. Lin, X.M Wu, Y. Kan, J.S. Zhu, Effect of Nd dopant on magnetic and electric properties of $BiFeO_3$ thin films prepared by metal organic deposition method, Appl. Phys. Lett. 89 (2006) 242914.

[11] B.F. Yu, M.Y. Li, J. Liu, D.Y. Guo, L. Pei, X.Z. Zhao, Effects of ion doping at different sites on electrical properties of multiferroic $BiFeO_3$ ceramics, J. Phys. D Appl. Phys. 41 (2008) 065003.

[12] Y. Wang, C.W. Nan, Effect of Tb doping on electric and magnetic behavior of $BiFeO_3$ thin films, J. Appl. Phys. 103 (2008) 024103.

[13] J. Liu, M.Y. Li, L. Pei, B.F. Yu, D.Y. Guo, X.Z. Zhao, Effect of Ce doping on the microstructure and electrical properties of $BiFeO_3$ thin films prepared by chemical solution deposition, J. Phys. D Appl. Phys. 42 (2009) 115409.

[14] J. Liu, M.Y. Li, L. Pei, J. Wang, B.F. Yu, X. Wang, X.Z. Zhao, Structural and multiferroic properties of the Ce-doped $BiFeO_3$ thin films, J. Alloys Compd. 493 (2010) 544.

[15] A. Lahmar, S. Habouti, M. Dietze, C.-H. Solterbeck, M. Es-Souni, Effects of rare earth manganites on structural, ferroelectric, and magnetic properties of $BiFeO_3$ thin films, Appl. Phys. Lett. 94 (2009) 012903.

[16] Y. Wang, C.W. Nan, Structural and ferroic properties of Zr-doped $BiFeO_3$ thin films, Ferroelectrics 357 (2007) 172.

[17] H. Naganuma, J. Miura, S. Okamura, Ferroelectric, electrical and magnetic properties of Cr, Mn, Co, Ni, Cu added polycrystalline $BiFeO_3$ films, Appl. Phys. Lett. 93 (2008) 052901.

[18] P. Kharel, S. Talebi, B. Ramachandran, A. Dixit, V.M. Naik, M.B. Sahana, C. Sudakar, R. Naik, M.S.R. Rao, G. Lawes, Structural, magnetic, and electrical studies on polycrystalline transition-metal-doped $BiFeO_3$ thin films, J. Phys. C Condens. Matter 21 (2009) 036001.

[19] J. Liu, M.Y. Li, L. Pei, J. Wang, Z.Q. Hu, X. Wang, X.Z. Zhao, Effect of Ce and Zr codoping on the multiferroic properties of $BiFeO_3$ thin films, Europhys. Lett. 89 (2010) 57004.

[20] G.L. Yuan, S.W. Or, Multiferroicity in polarized single-phase $Bi_{0.875}Sm_{0.125}FeO_3$, ceramics, J. Appl. Phys. 100 (2006) 024109.

[21] C.-H. Yang, J. Seidel, S.Y. Kim, P.B. Rossen, P. Yu, M. Gajek, Y.H. Chu, L.W. Martin, M.B. Holcomb, Q. He, P. Maksymovych, N. Balke, S.V. Kalinin, A.P. Baddorf, S.R. Basu, M.L. Scullin, R. Ramesh, Electric modulation of conduction in multiferroic Ca-doped $BiFeO_3$ films, Nature 8 (2009) 485.

[22] M. Fiebig, Revival of the magnetoelectric effect, J. Phys. D 38 (2005) R123.

[23] R. Ramesh, N.A. Spaldin, Multiferroics: progress and prospects in thin films, Nat. Mater. 6 (2007) 21.

[24] S.W. Cheong, M. Mostovoy, Multiferroics: a magnetic twist for ferroelectricity, Nat. Mater. 6 (2007) 13.

[25] H.W. Jang, S.H. Baek, D. Ortiz, C.M. Folkman, C.B. Eom, Y.H. Chu, P. Shafer, R. Ramesh, V. Vaithyanathan, D.G. Schlom, Epitaxial (001) $BiFeO_3$ membranes with substantially reduced fatigue and leakage, Appl. Phys. Lett. 92 (2008) 062910.

[26] T. Kawae, Y. Terauchi, H. Tsuda, M. Kumeda, A. Morimoto, Improved leakage and ferroelectric properties of Mn and Ti codoped $BiFeO_3$ thin films, Appl. Phys. Lett. 94 (2009) 112904.

[27] B.F. Yu, M.Y. Li, Z.Q. Hu, L. Pei, D.Y. Guo, X.Z. Zhao, S.X. Dong, Enhanced multiferroic properties of the high-valence Pr doped $BiFeO_3$ thin film, Appl. Phys. Lett. 93 (2008) 182909.

[28] V.A. Khomchenko, D.A. Kiselev, J.M. Vieira, A.L. Kholkin, M.A. Sá, Y. G. Pogorelov, Synthesis and multiferroic properties of $Bi_{0.8}A_{0.2}FeO_3$ (A=Ca,Sr,Pb) ceramics, Appl. Phys. Lett. 90 (2007) 242901.

[29] M.Y. Li, M. Ning, Y.G. Ma, Q.B. Wu, C.K. Ong, Room temperature ferroelectric, ferromagnetic and magnetoelectric properties of Ba-doped $BiFeO_3$ thin films, J. Phys. D: Appl. Phys. 40 (2007) 1603.

[30] J. Liu, M.Y. Li, Z.Q. Hu, L. Pei, J. Wang, X.L. Liu, X.Z. Zhao, Effects of ion-doping at different sites on multiferroic properties of $BiFeO_3$ thin films, Appl. Phys. A—Mater. 102 (2011) 713.

[31] O.D. Jayakumar, S.N. Achary, K.G. Girija, A.K. Tyagi, C. Sudakar, G. Lawes, R. Naik, J. Nisar, X. Peng, R. Ahuja, Theoretical and experimental evidence of enhanced ferromagnetism in Ba and Mn cosubstituted $BiFeO_3$, Appl. Phys. Lett. 96 (2010) 032903.

[32] N. Hiroshi, O. Tomosato, S. Sho, A. Yasuo, O. Soichiro, Structural, magnetic, and ferroelectric properties of multiferroic $BiFeO_3$-based composite films with exchange bias, J. Appl. Phys. 105 (2009) 07D903.

[33] S. Jo, S.G. Lee, S.H. Lee, Structural and pyroelectric properties of sol–gel derived multiferroic $BiFeO_3$ thin films, Mater. Res. Bull. 47 (2012) 409.

[34] J. Wang, A. Scholl, H. Zheng, S.B. Ogale, D. Viehland, D.G. Schlom, N.A. Spaldin, K.M Rabe, M Wuttig, L. Mohaddes, J. Neaton, U. Waghmare, T. Zhao, R. Ramesh, Response to comment on epitaxial $BiFeO_3$ multiferroic thin film heterostructures, Science 307 (2005) 1203b.

[35] C. Ederer, N.A. Spaldin, Influence of strain and oxygen vacancies on the magnetoelectric properties of multiferroic bismuth ferrite, Phys. Rev. B: Condens. Matter 71 (2005) 224103.

[36] K. Ueda, H. Tabata, T. Kawai, Coexistence of ferroelectricity and ferromagnetism in $BiFeO_3$–$BaTiO_3$ thin films at room temperature, Appl. Phys. Lett. 75 (1999) 555.

[37] B.H. Park, B.S. Kang, S.D Bu, T.W. Noh, J. Lee, W. Jo, Lanthanum-substituted bismuth titanate for use in non-volatile memories, Nature 401 (1999) 682.

[38] M.-W. Chu, M. Ganne, M.T. Caldes, E. Gautier, L. Brohan, X-ray photoemission spectroscopy characterization of the electrode-ferroelectric interfaces in $Pt/Bi_4Ti_3O_{12}/Pt$ and $Pt/Bi_{3.25}La_{0.75}Ti_3O_{12}/Pt$ capacitors: possible influence of defect structure on fatigue properties, Phys. Rev. B 68 (2003) 14102.

[39] L.V. Costa, R.C. Deus, C.R. Foschini, E. Longo, M. Cilense, A.Z. Simões, Experimental evidence of enhanced ferroelectricity in Ca doped $BiFeO_3$, Mater. Chem. Phys. 144 (2014) 476.

[40] A.Z. Simões, A.H.M. Gonzalez, L.S Cavalcante, C.S. Riccardi, E. Longo, J.A. Varela, Soft chemical deposition of $BiFeO_3$ multiferroic thin films, Appl. Phys. Lett. 90 (2007) 052906.

[41] R.A. Young, A. Sakthivel, T.S. Moss, C.O. Paiva-Santos, *DBWS*-9411—an upgrade of the *DBWS*✻.✻ programs for Rietveld refinement with PC and mainframe computers, J. Appl. Crystallogr. 28 (1995) 366–367.

[42] H.M. Rietveld, A profile refinement method for nuclear and magnetic structures, J. Appl. Crystallogr. 2 (1969) 65.

[43] D.L. Bish, J.E. Post, Quantitative mineralogical analysis using the Rietveld full-pattern fitting method, Am. Mineral. 78 (1993) 932.

[44] ⟨http://www.ing.unitn.it/∼maud/⟩.

[45] L. Lutterotti, S. Matthies, H.-R. Wenk, A.J. Schultz, J.J. Richardson, Texture and structure analysis of deformed limestone from neutron diffraction spectra, Appl. Phys. 81 (1997) 594.

[46] G. Will, Powder Diffraction: the Rietveld Method and the Two Stage Method to Determine and Refine Crystal Structures from Powder Diffraction Data, Springer-Verlag, Berlin, Heidelberg, 2006, p. 44–69.

[47] T. Barth, G. Lunde, Lattice constants of the cuprous and silver halides, Z. Phys. Chem. 121 (1926) 78.

[48] C. Lepoittevin, S. Malo, N. Barrier, N. Nguyen, G. Van. Tendeloo, M. Hervieu, Long-range ordering in the $Bi_{1-x}Ae_xFeO_{3-x/2}$ perovskites: $Bi_{1/3}Sr_{2/3}FeO_{2.67}$ and $Bi_{1/2}Ca_{1/2}FeO_{2.75}$, J. Solid State Chem. 181 (2008) 2601.

[49] S.K. Singh, K. Maruyama, H. Ishiwara, The influence of La-substitution on the micro-structure and ferroelectric properties of chemical-solution-deposited $BiFeO_3$ thin films, J. Phys. D: Appl. Phys. 40 (2007) 2705.

[50] H. Liu, Z. Liu, K. Yao, Improved electric properties in $BiFeO_3$ films by the doping of Ti, J. Sol–Gel Sci. Technol. 41 (2007) 123.

[51] X.J. Meng, J.G. Cheng, J.L. Sun, H.J. Ye, Growth of (1 0 0)-oriented $LaNiO_3$ thin films directly on Si substrates by a simple metalorganic decomposition technique for the highly oriented PZT thin films, J. Cryst. Growth 220 (2000) 100.

[52] W. Zhu, M.S. Tse, W. Lu, Raman, X-ray and electrical properties of MOD PZT/PLZT thin films, Integr. Ferroelectr. 12 (1996) 167.
[53] S.K. Singh, H. Ishiwara, K. Maruyama, Room temperature ferroelectric properties of Mn-substituted $BiFeO_3$ thin films deposited on Pt electrodes using chemical solution deposition, Appl. Phys. Lett. 88 (2006) 262908.
[54] G.D. Hu, X. Cheng, W.B Wu, C.H. Yang, Effects of Gd substitution on structure and ferroelectric properties of $BiFeO_3$ thin films prepared using metal organic decomposition, Appl. Phys. Lett. 91 (2007) 232909.
[55] H. Uchida, R. Ueno, H. Funakubo, S. Koda, Crystal structure and ferroelectric properties of rare-earth substituted $BiFeO_3$ thin films, J. Appl. Phys. 100 (2006) 014106.
[56] Y. Wang, C.W. Nan, Enhanced ferroelectricity in Ti-doped multiferroic $BiFeO_3$ thin films, Appl. Phys. Lett. 89 (2006) 052903.
[57] F. Gao, C. Cai, Y. Wang, S. Dong, X.Y. Qiu, G.L. Yuan, Z.G. Liu, J.-M. Liu, Preparation of La-doped BiFeO thin films with Fe^{2+} ions on Si substrates, J. Appl. Phys. 99 (2006) 094105.
[58] S.R. Shannigrahi, A. Huang, N. Chandrasekhar, Sc modified multiferroic $BiFeO_3$ thin films prepared through a sol–gel process, Appl. Phys. Lett. 90 (2007) 022901.
[59] C. Wang, M. Takahashi, H. Fujino, X. Zhao, E. Kume, T. Horiuchi, S. Sakai, Leakage current of multiferroic $(Bi_{0.6}Tb_{0.3}La_{0.1})FeO_3$ thin films grown at various oxygen pressures by pulsed laser deposition and annealing effect, J. Appl. Phys. 99 (2006) 054104.
[60] H. Yang, Y.Q. Wang, H. Wang, Q.X. Jia, Oxygen concentration and its effect on the leakage current in $BiFeO_3$ thin films, Appl. Phys. Lett. 96 (2010) 012909.